

Tribological behavior of carbon nanotube composite coatings on C/C composite

Jeong-Wook An^a and Dae-Soon Lim^{a,b,*}

^aDepartment of Materials Science and Engineering, Korea University, Seoul 136-701, Korea

^bCeramic Processing Research Center, Hanyang University, Seoul 133-791, Korea

Carbon nanotube (CNT) composite coatings were applied onto C/C composites to improve their wear behavior. CNT was synthesized by catalytic decomposition of acetylene gas. The nanotube slurry was prepared by mixing CNT, phenolic resin and methanol to deposit on and infiltrate into the C/C composites. The CNT composite coatings on C/C composites were carbonized in a nitrogen atmosphere. The tribological properties were determined using a ball on disk type wear tester. The results showed that the CNT composite coating decreased the wear rate significantly and increased the friction coefficient slightly.

Key words: Carbon nanotube (CNT), C/C composite, Composite coating, Wear.

Introduction

Carbon fiber reinforced carbon (C/C) composites possess excellent high temperature mechanical properties and low density as well as good wear and frictional properties. Therefore, they are considered to be good candidate materials for tribological applications such as nozzles, and aircraft brake disks and linings [1-3]. Although C/C composites have been used in some tribological applications, the understanding of their friction and wear behavior is very limited because very few studies on the tribological behavior of C/C composites have been published [4, 5]. In inert environments, the friction of carbon materials shows a high value and the wear rate can reach 10^4 times higher than that in air [6-8]. Under the conditions of heavy load and high speed, the wear rate becomes apparently higher [4]. Previous researchers also reported that the types of the matrix and fiber could affect the tribological behavior of C/C composites [9, 10]. All the aforementioned studies have suggested that the friction and wear properties of C/C composites should be improved in order to expand their tribological applications.

In the present study, carbon nanotube (CNT) layers were coated on C/C composites to improve the tribological performance. CNT was selected since it has unique mechanical properties that make it a promising candidate for mechanical reinforcements [11]. Recently, preliminary studies have been carried out on carbon nanotube composites with polymers, metals and ceramics to improve their mechanical and electrical properties

[12-15]. However, information regarding the tribological performance of carbon nanotubes has not previously been available. This paper presents the results of an investigation of carbon nanotube infiltration on the tribological performance of C-C composites.

Experimental Procedure

CNTs were produced by the catalytic decomposition of C_2H_2 using a tube furnace which can be operated up to a temperature of $1200^\circ C$ at atmospheric pressure (Fig. 1). The experimental set-up is somewhat like that reported elsewhere [16]. The CNTs were grown using a gas mixture of C_2H_2 , H_2 , $Fe(CO)_5$ with N_2 as a carrier gas. After synthesis, the CNTs on the inner wall of the inner quartz tube were collected.

The collected CNTs were examined by a SEM (Hitachi, S-4300) and TEM (Hitachi, H9000-NAR) to measure the length, diameter and uniformity. HRTEM was used to determine the wall structure of individual carbon nanotubes. Micro-Raman experiments were carried out with a Raman spectrophotometer (Jobin Yvon, T64000) in an ambient atmosphere and at room temperature.

A Composite of uniformly mixed carbon fiber and phenolic resin was hot-pressed at a pressure of 20 MPa at $150^\circ C$ for 3 hr. The composite was cut to dimensions of $15\text{ mm} \times 15\text{ mm}$ and subjected to a carbonization process by heating to $1000^\circ C$ at a heating rate of 2 K/minute under a nitrogen atmosphere. The hold time at $1000^\circ C$ was 2 hr.

Four different slurries were prepared with the CNT contents ranging from 0 to 20 wt.%. The CNTs were added to the solution of the phenolic resin and methanol (1:1 by weight). Then the carbonized C/C composites were immersed in each slurry and dried at

*Corresponding author:
Tel : +82-2-3290-3272
Fax: +82-2-929-5344
E-mail: dslim@korea.ac.kr

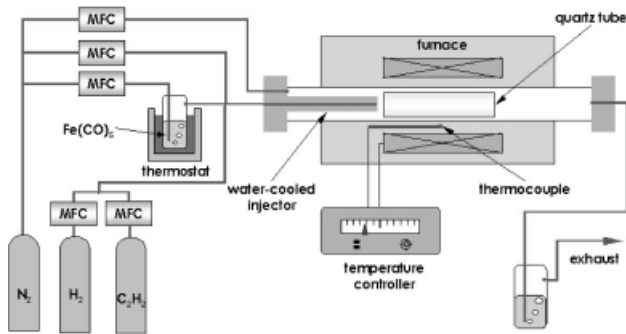


Fig. 1. Schematic of the reactor used for the CNT synthesis.

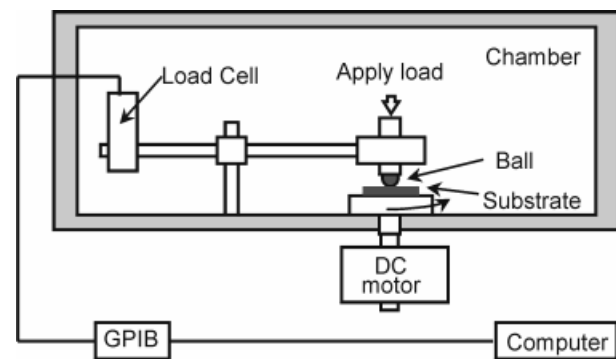


Fig. 2. Schematic diagram of wear tester.

room temperature for 24 hrs. The dried samples were carbonized again according to the previously described carbonization process.

Ball-on-disk type wear tests were performed to evaluate the tribological properties of the CNT coated C/C composites. Figure 2 shows a schematic diagram of the wear tester. The silicon nitride ball used was a commercially available bearing grade ball, and its diameter was 6.35 mm. The normal load and sliding speed were fixed at 1.5 N and 0.5 m/s respectively. The test duration was 1 hr. The frictional force transferred to a load cell was recorded throughout the tests. The load cell produced an electrical output depending on the frictional force. The electrical signal amplified by a multimeter was stored in a computer *via* a general-purpose interface bus (GPIB). After the wear tests, the worn and un-worn surfaces of each sample were examined with an SEM.

Results and Discussion

Soot-like deposits were formed on the entire inner-wall of the quartz tube after the catalytic pyrolysis of the hydrocarbon at 750°C for 60 minutes. Figure 3 shows an SEM image of the collected soot-like deposits without any purification process. The tubes have a diameter of about 10-50 nm, while their length is about 3-5 μm. HRTEM was used to observe the interior and wall structures of the CNTs. Figure 4a shows a typical TEM micrograph of the CNTs. This clearly shows that

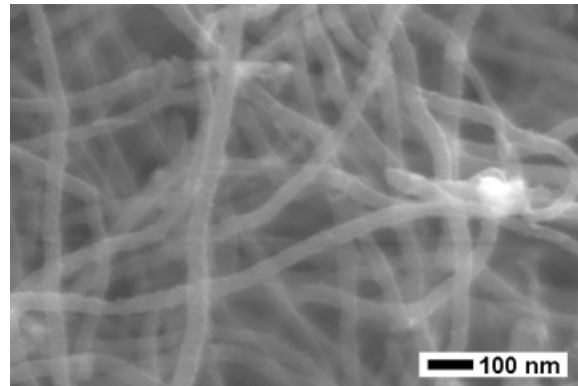
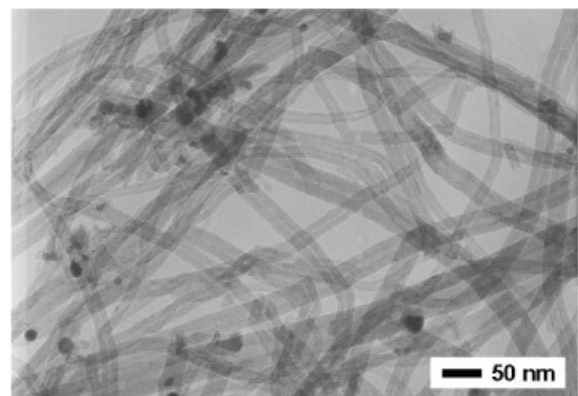
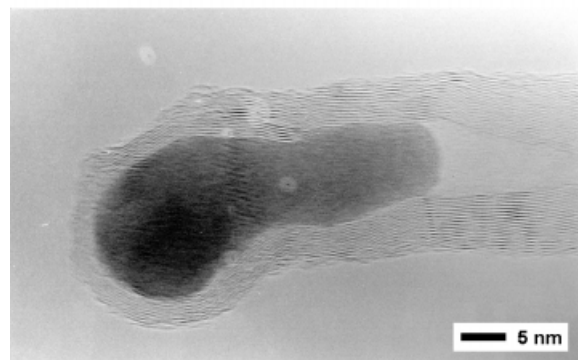


Fig. 3. SEM image of the CNT produced by the catalytic pyrolysis of hydrocarbon (C₂H₂) at 750°C for 60 min.



(a)



(b)

Fig. 4. (a) TEM image of CNTs dispersed on a carbon grid. (b) HRTEM image of multi-walled CNT with a catalytic particle encapsulated in the tip.

the nanotube is a multi-walled hollow tube, not a solid fiber. Also, most of the closed tips are filled with iron particles. Figure 4b is a HRTEM image of a single CNT and tip structure. This shows the inside hollow with a diameter of 3-5 nm. The fringes on each side of the tube represent individual cylindrical graphitic layers. An iron nanoparticle is encapsulated at the end of the nanotube. This indicates that the iron catalyst particles promote the tip growth process and play an essential role in the formation of the nanotubes as suggested by

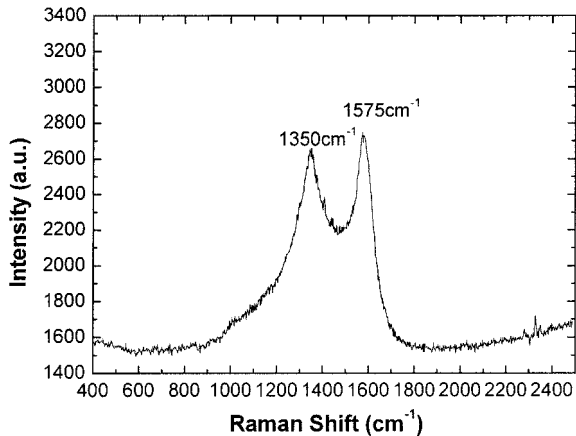


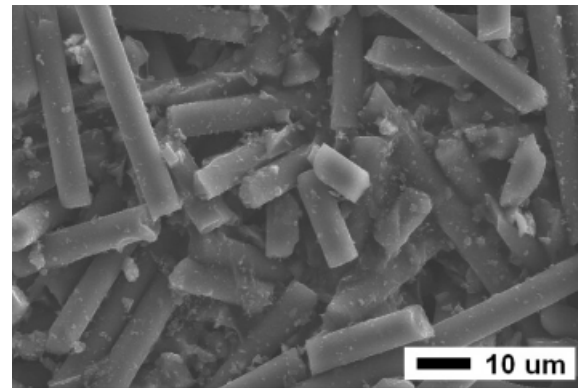
Fig. 5. Micro-Raman spectra obtained from as-grown multi-walled CNTs.

other researchers [17-18].

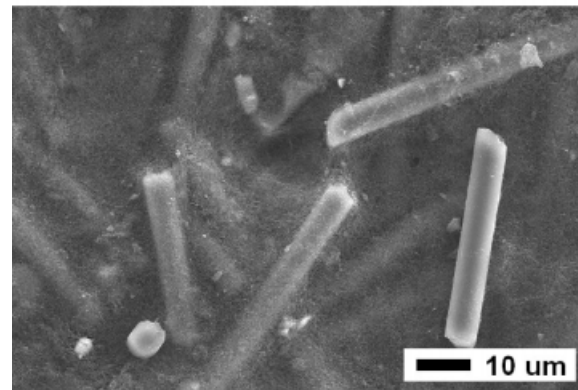
Micro-Raman spectra were obtained for the as-grown CNT (Fig. 5). In the Raman spectra obtained from as-grown multi-walled CNT, two dominating optically active phonon modes are shown. The line at 1575 cm^{-1} is a G-line and is the optically active in-plane stretching E_{2g} mode. And the D-line at 1350 cm^{-1} is a disorder-induced line where the selection rules break down due to a defect state (defects in the nanotube and tube curvature) present [19-20].

The C/C composite, which was produced by carbonization of the carbon fiber/phenolic resin composite at 1000°C for 2 hours, had a bulk density of 0.8869 g/cm^3 . The carbon nanotube coatings were produced by CNT slurry infiltration into the C/C composite and a carbonization process. Fig. 6 shows typical surface morphologies of 0, 5 and 20 wt.% CNT added composites. Fig. 6a shows the surface morphology of a 0% CNT added specimen. It is seen that the fibers are randomly oriented. For the 5% CNT solution coated composite, the surface was partially covered with a CNT/carbon layer. As the CNT addition was raised to 20%, the whole surface was covered with a CNT/carbon layer. Fig. 7 shows a higher magnification SEM micrographs of a 0% and 20% CNT added specimen surfaces. It is seen that the CNT are highly cross-linked and randomly oriented (Fig. 7b). An SEM image of the fractured 20% CNT added specimen is shown in Fig. 8. The thickness of the coating layer is about $20\text{ }\mu\text{m}$. The inset shows a magnified image of the CNT/carbon composite layer. It shows that the CNT keeps its shape after the carbonization process.

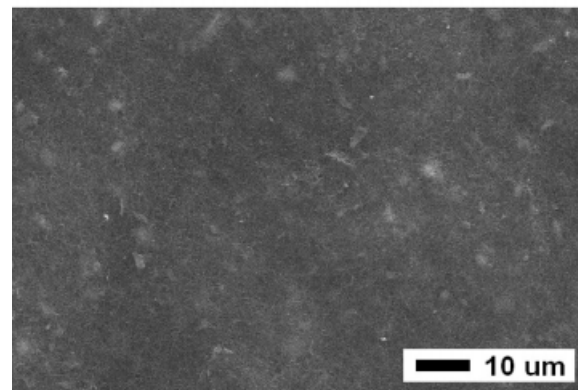
The variations of wear loss and friction coefficient as a function of CNT addition are shown in Fig. 9. It is seen that the friction coefficient increased as the CNT additions increased. The weight loss from the 5% CNT added composite is decreased by nearly 30% as compared to that of the 0% CNT (100% phenolic resin) added composite. As the CNT concentrations are increased up to 20%, the weight losses decrease



(a)



(b)



(c)

Fig. 6. SEM micrographs of C/C composites infiltrated with various concentrations of CNT solution and carbonized. (a) 0 weight % CNT solution, (b) 5 weight % CNT solution and (c) 20 weight % CNT solution.

gradually. SEM micrographs of worn surfaces after wear tests are shown in Fig. 10. For all specimens, the worn surfaces are covered with a thick layer of wear debris and fractured carbon fibers are also observed. As the CNT additions are increased, flatter and thicker layers of wear debris are observed. The increase of the friction coefficient by CNT addition might be due to the superior mechanical properties of CNTs. Rao *et al.* reported that isotropic pitch composite fibers prepared with a few weight percent loading of CNTs yield composite materials with enhanced tensile strength and

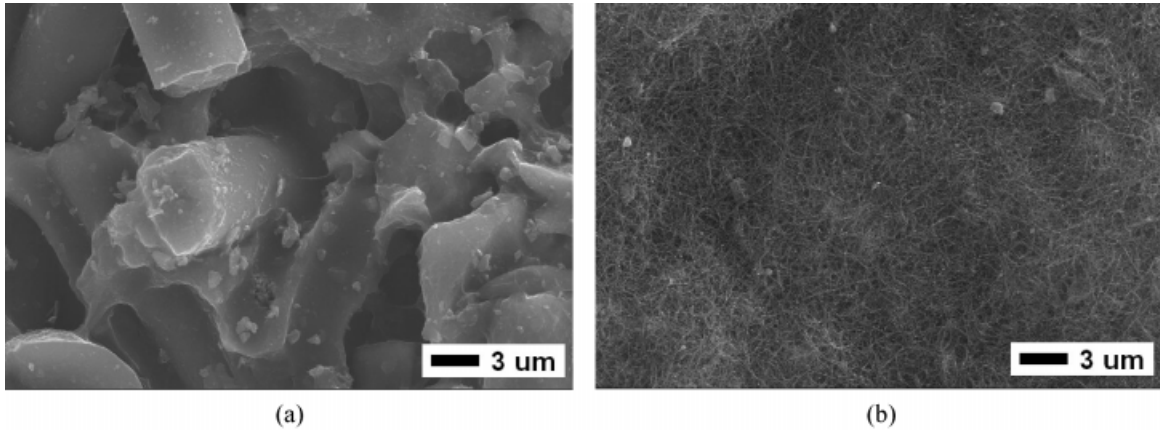


Fig. 7. High-resolution SEM images of (a) Fig. 4a and (b) Fig. 4c.

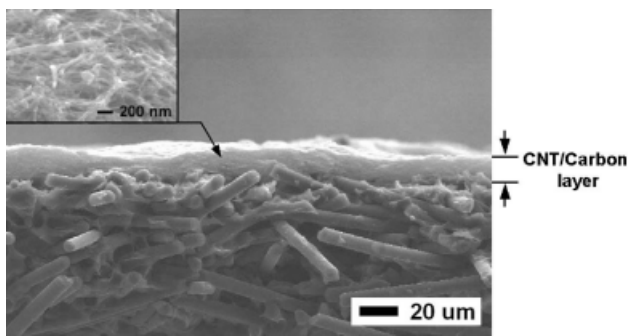


Fig. 8. SEM image of a fractured 20% CNT added specimen. Inset shows magnified view of the CNT/carbon layer.

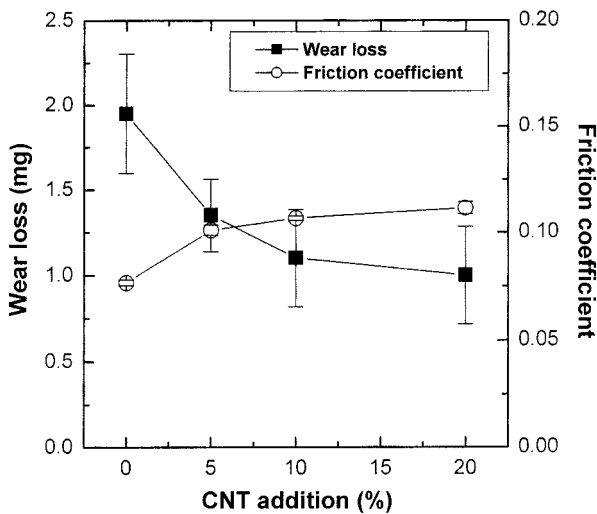


Fig. 9. Variations of weight loss and friction coefficient as a function of CNT addition after wear tests.

modulus [21-22]. The wear resistance of the 20% CNT coated C/C composite was improved by about 100% as compared to that of the 0% CNT coated C/C composite. More work is needed to understand the detailed mechanism for the CNT addition effect on the tribological performance.

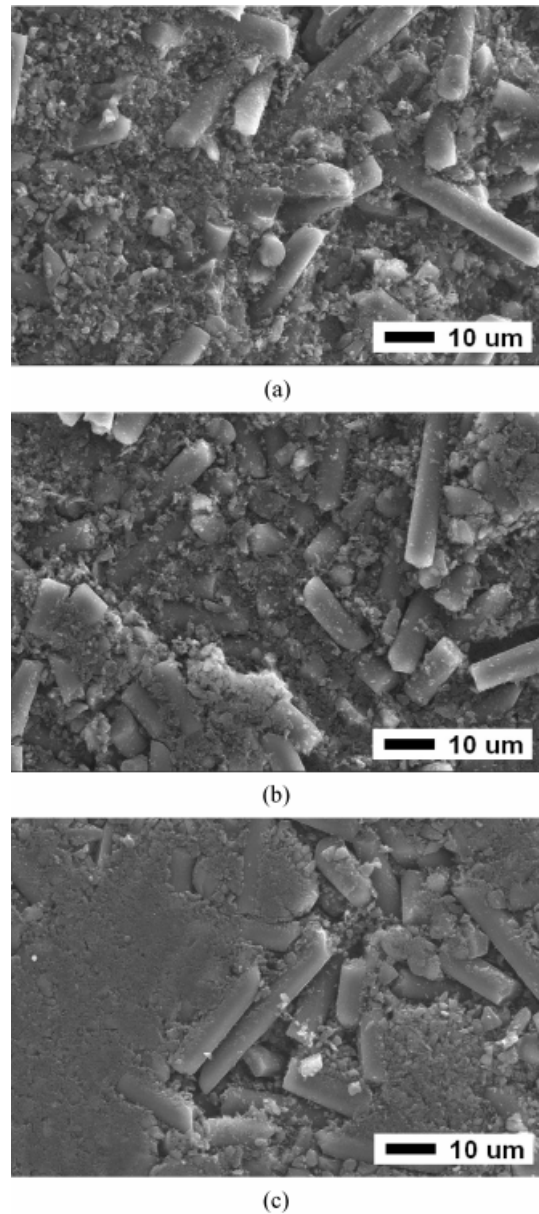


Fig. 10. SEM micrographs of worn surfaces of C/C composites infiltrated with (a) 0% CNT solution, (b) 5% CNT solution and (c) with 20% CNT solution.

Conclusions

CNT/carbon composite layers with CNT contents ranging from 0 to 20% were fabricated and coated on C/C composites to improve their wear resistance. The CNT/carbon composite layers were obtained by infiltration of slurries mixed with multi-walled CNT obtained by catalytic decomposition. Wear loss decreased significantly but the friction coefficient slightly increased as the CNT addition increased. The enhanced wear properties are a result of the multi-walled CNT's behavior in reinforcing the filler in the coated layer and within the carbon fibers.

Acknowledgements

This work was supported by the Ceramic Processing Research Center (CPRC) through a grant of the Korea Science and Engineering Foundation.

References

1. I.L. Stimson, and R. Fisher, *Philos. Trans. R. Soc. London A* 294 (1980) 583-590.
2. E. Fitzer, *Carbon* 25 (1987) 163-190.
3. G. Savage, in "Carbon-Carbon Composites" (Chapman and Hall, 1993) p.323.
4. B.K. Yen, and T. Ishihara, *Wear* 174 (1994) 111-117.
5. C. Blanco, J. Bermejo, H. Marsh, and R. Menendez, *Wear* 213 (1997) 1-12.
6. B.K. Yen, *Wear* 192 (1996) 208-215.
7. N. Murdie, C.P. Ju, J. Don, and F.A. Fortunato, *Carbon* 29 (1991) 335-342.
8. B.K. Yen, *J. Mater. Sci. Lett.* 14 (1995) 1481-1483.
9. S. Awasthi, and J.L. Wood, *Adv. Ceram. Mater.* 3 (1988) 449-451.
10. C.P. Ju, K.J. Lee, H.D. Wu, and C.I. Chen, *Carbon* 32 (1994) 971-978.
11. T.W. Ebbesen, in "Carbon Nanotubes" (CRC Press, 1997) p.277.
12. Ch. Laurent, A. Peigney, E. Flahaut, and A. Rousset, *Mater. Res. Bull.* 35 (2000) 661-673.
13. J. Sandler, M.S.P. Shaffer, T. Prasse, W. Bauhofer, K. Schulte, and A.H. Windle, *Polymer* 40 (1999) 5967-5971.
14. X. Chen, J. Xia, J. Peng, W. Li, and S. Xie, *Compos. Sci. Technol.* 60 (2000) 301-306.
15. C.A. Grimmes, C. Mungle, D. Kouzoudis, S. Fang, and P.C. Eklund, *Chem. Phys. Lett.* 319 (2000) 460-464.
16. F. Rohmund, L.K.L. Falk, and E.E.B. Campbell, *Chem. Phys. Lett.* 328 (2000) 369-373.
17. S. Amelinckx, X.B. Zhang, D. Bernaerts, X.F. Zhang, V. Ivanov, and J.B. Nagy, *Science* 265 (1994) 635-639.
18. S.B. Sinnott, R. Andrews, D. Qian, A.M. Rao, Z. Mao, E.C. Dickey, and F. Derbyshire, *Chem. Phys. Lett.* 315 (1999) 25-30.
19. R.J. Nemanich, and S.A. Solin, *Phys. Rev. B* 20 (1979) 392-401.
20. A.M. Rao, E. Richer, S. Bandow, B. Chase, P.C. Eklund, K.A. Williams, S. Fang, K.R. Subbaswamy, M. Menon, A. Thess, R.E. Smally, G. Dresselhaus, and M. S. Dresslhaus, *Science* 275 (1997) 187-191.
21. A.M. Rao, R. Andrews, and F. Derbyshire, *Energeia* 9 (1998) 1-6.
22. R. Andrews, D. Jacques, A.M. Rao, T. Rantell, F. Derbyshire, Y. Chen, J. Chen, and R.C. Haddon, *Appl. Phys. Lett.* 75 (1999) 1329-1331.